SUPPLEMENTAL FIGURES

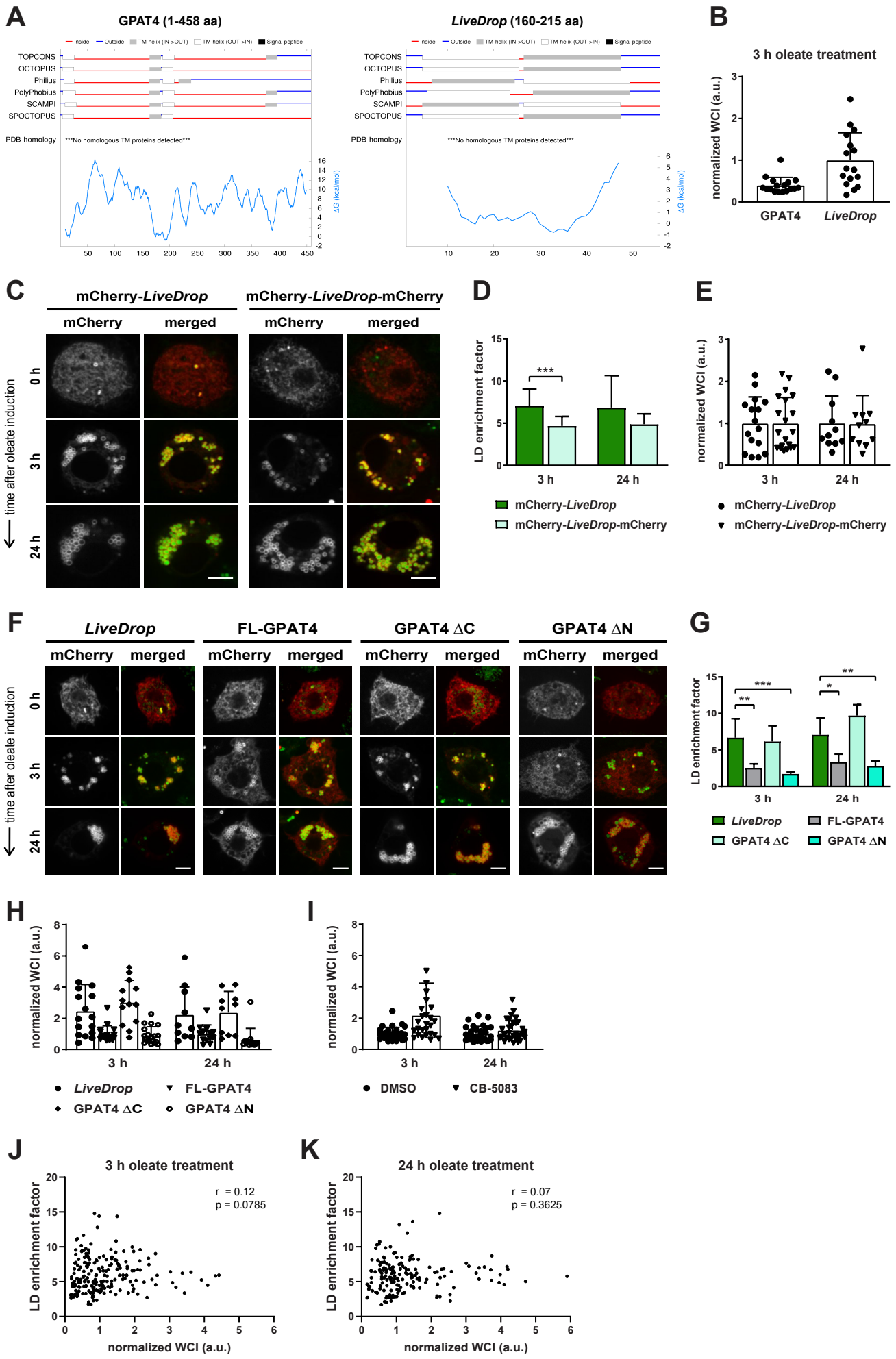

Figure S1 (related to Figure 1). The different timing of LD targeting for full-length GPAT4 and *LiveDrop* is mediated by a C-terminal segment of the full-length protein

(A) Secondary structure predictions of *D. melanogaster* GPAT4 (1–458 aa, left) and the *LiveDrop* motif (160–215 aa, right). TOPCONS (http://topcons.cbr.su.se/) was used to predict the transmembrane (TM) domains in both sequences. The results also include the predictions from additional bioinformatics tools, such as OCTOPUS, Philius, PolyPhobius, SCAMPI, and SPOCTOPUS. The predicted TM domains are depicted as white and gray bars, based on their membrane orientation, and the sequence regions predicted to be non-TM are represented as solid lines. The results of comparing each sequence to the PDB (Protein Data Bank), as well as the respective free energy (∆G kcal/mol) profiles (blue trace), are shown at the bottom of each panel.
(B) Mean values + SD (n > 15) of the whole-cell protein signals for the cells expressing GPAT4 and *LiveDrop* in Figs. 1B and 1C. Single data points are shown. WCI, whole-cell intensity; a.u., arbitrary units.
(C) The early targeting of *LiveDrop* to nascent LDs is not due to deficient ER retention. *Drosophila* S2 cells were transfected with mCherry-tagged *LiveDrop* or with a similar construct bearing an additional C-terminal mCherry fluorophore (red). Cells were incubated with oleate throughput the indicated time points and imaged by confocal microscopy. LDs were stained with BODIPY (green). Scale bar, 5 µm.
(D) Mean values + SD (n > 11) of the protein signal on LDs after 3 and 24 h of oleate treatment. ***, $p < 0.001$.
(E) Mean values + SD (n > 11) of the whole-cell protein signals for the cells expressing *LiveDrop* and the indicated protein variant in Figs. S1C and S1D. Single data points are shown. WCI, whole-cell intensity; a.u., arbitrary units.
(F) A C-terminal segment of full-length GPAT4 delays the LD targeting of *LiveDrop*. *Drosophila* S2 cells were transfected with mCherry-tagged versions of *LiveDrop*, full-length GPAT4 (FL-GPAT4), and the truncations GPAT4 ∆C (1-215 aa) and GPAT4 ∆N (160-458 aa) (red). Cells were incubated with oleate throughout the indicated time points and imaged by confocal microscopy. LDs were stained with BODIPY (green). Scale bar, 5 µm.
(G) Mean values + SD (n > 10) of the protein signal on LDs after 3 and 24 h of oleate treatment. *, $p < 0.05$; **, $p < 0.01$; ***, $p < 0.001$.
(H) Mean values + SD (n > 10) of the whole-cell protein signals for the cells expressing *LiveDrop*, FL-GPAT4, and the GPAT4 truncations in Figs. S1F and S1G. Single data points are shown. WCI, whole-cell intensity; a.u., arbitrary units.
(I) Mean values + SD (n > 23) of the whole-cell protein signals for the cells expressing *LiveDrop* in Figs. 1F and 1G. Single data points are shown. WCI, whole-cell intensity; a.u., arbitrary units.
(J) and **(K)** The enrichment of *LiveDrop* on LDs does not correlate with its expression levels. Plots of the LD enrichment factors measured for *LiveDrop*, across different experiments, against its corresponding whole-cell intensity (WCI) values. After 3 h of oleate treatment **(J)**, no statistical correlation was identified between the two variables ($r = 0.12$, $n = 207$, $p = 0.0785$). Consistently, after 24 h of oleate treatment **(K)**, the variables showed no correlation ($r = 0.07$, $n = 171$, $p = 0.3625$). r, Spearman correlation coefficient; a.u., arbitrary units.

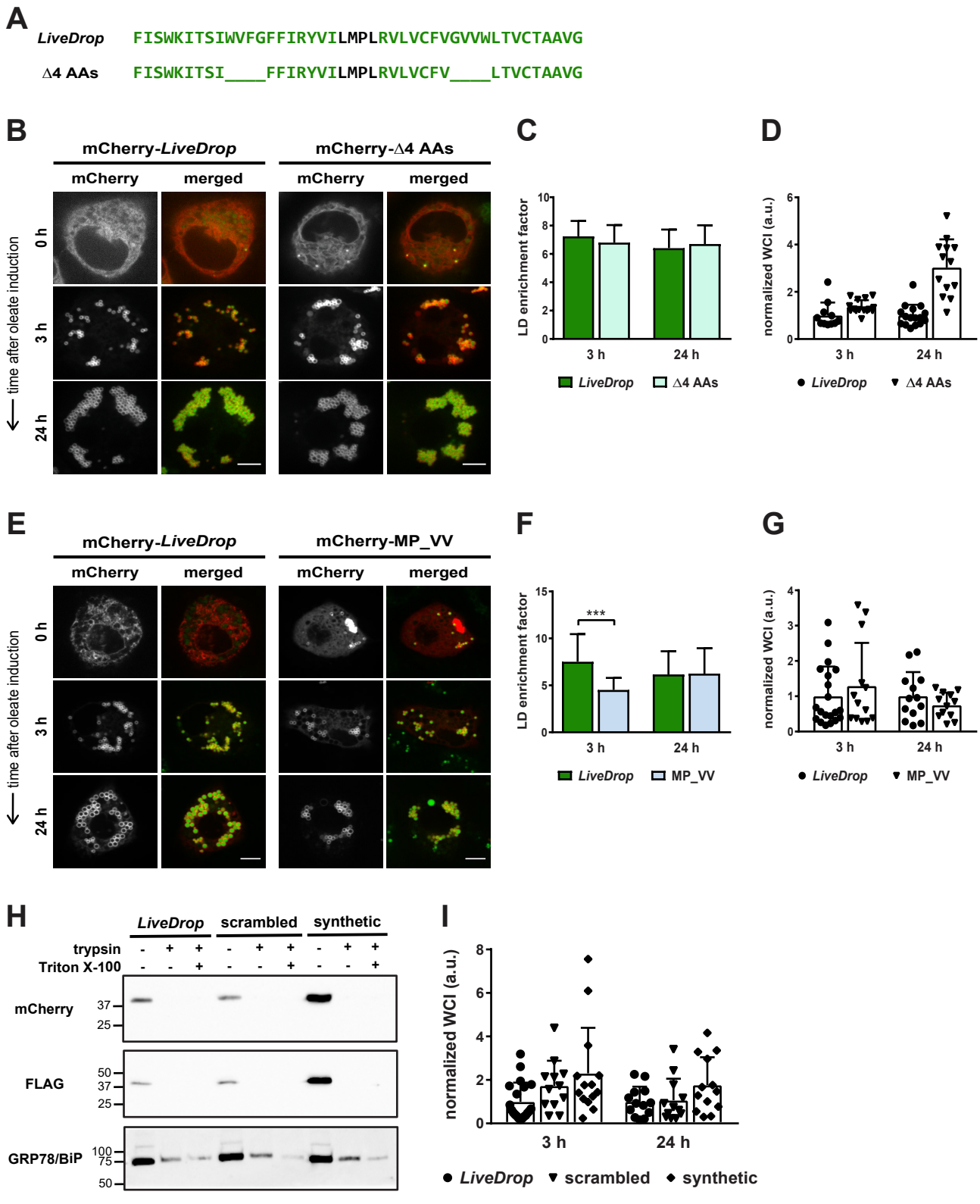
A
LiveDrop FISWKITSIWVFGFFIRYVILMPLRVLVCFVGVVWLTVCTAAVG
Δ4 AAs FISWKITSI____FFIRYVILMPLRVLVCFV____LTVCTAAVG
B
mCherry-LiveDrop
mCherry-Δ4 AAs
mCherry
merged
mCherry
merged
time after oleate induction
0 h
3 h
24 h
C
LD enrichment factor
3 h
24 h
LiveDrop
Δ4 AAs
D
normalized WCI (a.u.)
3 h
24 h
LiveDrop
Δ4 AAs
E
mCherry-LiveDrop
mCherry-MP_VV
mCherry
merged
mCherry
merged
time after oleate induction
0 h
3 h
24 h
F
LD enrichment factor
***
3 h
24 h
LiveDrop
MP_VV
G
normalized WCI (a.u.)
3 h
24 h
LiveDrop
MP_VV
H
LiveDrop
scrambled
synthetic
trypsin
Triton X-100
mCherry
FLAG
GRP78/BiP
37
25
50
37
25
100
75
50
I
normalized WCI (a.u.)
3 h
24 h
LiveDrop
scrambled
synthetic

Figure S2 (related to Figure 2). Disrupting global, structural features of *LiveDrop* does not preclude its LD targeting

(A) Amino acid sequence of *LiveDrop* and the Δ4 AAs variant (green), in which four amino acids were removed from the middle of both α-helices. The predicted hinge of both sequences is shown in black.
(B) Shortening the length of the transmembrane α-helices of *LiveDrop*, as is the case of the Δ4 AAs variant, does not affect LD targeting.
(C) Mean values + SD (n > 11) of the protein signal on LDs after 3 and 24 h of oleate treatment. No significant difference was observed between protein variants at either time point of LD induction.
(D) Mean values + SD (n > 11) of the whole-cell protein signals for the cells expressing *LiveDrop* and the Δ4 AAs variant in Figs. S2B and S2C. Single data points are shown. WCI, whole-cell intensity; a.u., arbitrary units.
(E) The residues located at the predicted hinge of *LiveDrop* are not required for LD targeting. A *LiveDrop* variant in which the midpoint residues methionine 184 (M184) and proline 185 (P185) are exchanged for valines (MP_VV) targets LDs similar to the wild-type sequence, except for a slight reduction at the 3 h time point of LD induction.
(F) Mean values + SD (n > 12) of the protein signal on LDs after 3 and 24 h of oleate treatment. ***, $p < 0.001$.
(G) Mean values + SD (n > 12) of the whole-cell protein signals for the cells expressing *LiveDrop* and the MP_VV variant in Figs. S2E and S2F. Single data points are shown. WCI, whole-cell intensity; a.u., arbitrary units.
For **(B)** and **(E)**, *Drosophila* S2 cells were transfected with mCherry-tagged versions of each of the *LiveDrop* variants (red), incubated with oleate throughout the indicated time points, and imaged by confocal microscopy. LDs were stained with BODIPY (green). Scale bar, 5 μm.
(H) The N- and C-termini of *LiveDrop*, its scrambled variant, and the synthetic hydrophobic motif are exposed to the cytosolic side of the ER membrane, consistent with a hairpin conformation. Microsomal fractions from *Drosophila* S2 cells expressing double-tagged versions of *LiveDrop* (mCherry-*LiveDrop*-FLAG), its scrambled variant (mCherry-scrambled-FLAG), and the synthetic hydrophobic motif (mCherry-synthetic-FLAG) were treated with 12.5 μg/ml of the protease trypsin in the absence or presence of 1% Triton X-100. Western blot analysis revealed that, in all cases, both the mCherry and FLAG tags were fully digested regardless of the presence of Triton X-100, while the ER luminal protein GRP78/BiP (control) only gets fully digested when including Triton X-100.
(I) Mean values + SD (n > 12) of the whole-cell protein signals for the cells expressing *LiveDrop*, its scrambled variant, and the synthetic hydrophobic motif in Figs. 2C and 2D. Single data points are shown. WCI, whole-cell intensity; a.u., arbitrary units.

A

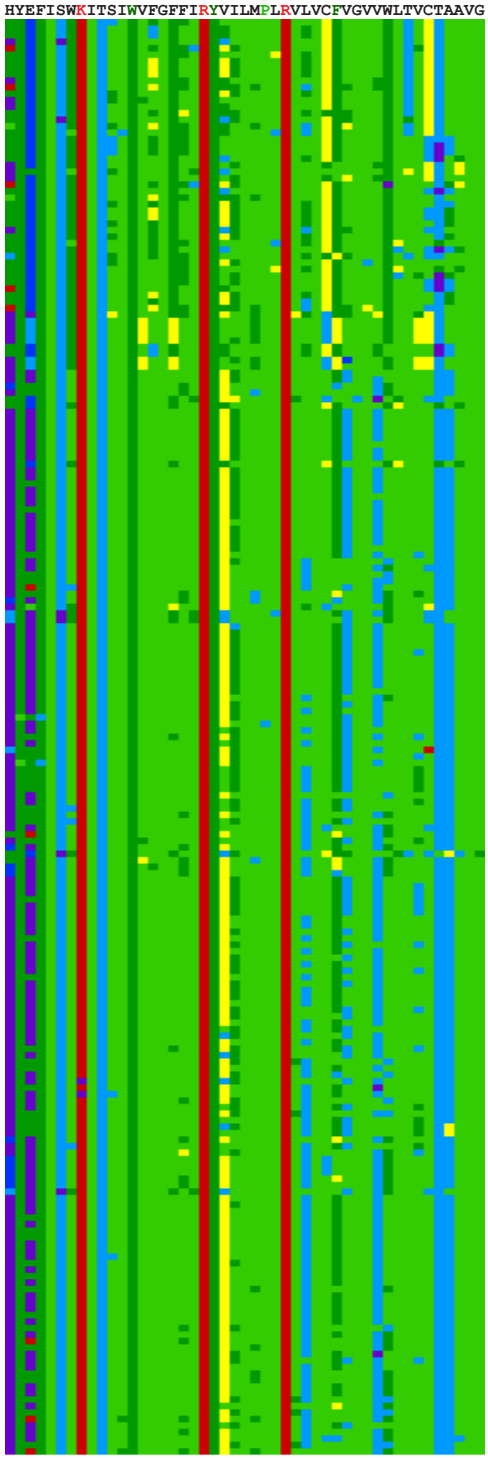
HYEFISWKITSIWVFGFFIRYVILMPLRVLVCFVGVVWLTVCTAAVG

B

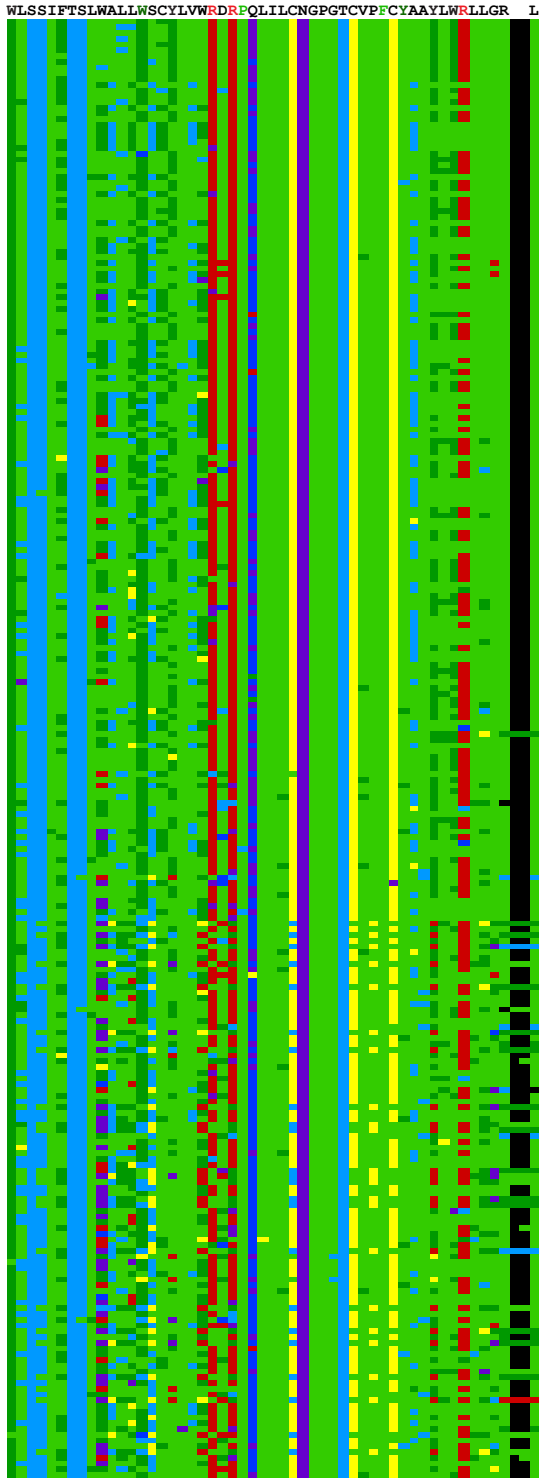
WLSSIFTSLWALLWSCYLVWRDRPQLILCNGPGTCVPFCYAAYLWRLLGR L

Figure S3 (related to Figures 2 and 5). Conservation profiles of the residues in the *LiveDrop* and ALG14 hairpin sequences

For both *LiveDrop* **(A)** and the predicted ALG14 hairpin **(B)**, high-throughput sequence alignments were performed and the corresponding results are depicted as conservation color maps. Within these maps, each row represents a different ortholog sequence (with an identity above 40%) and the columns represent each of the amino acid positions in the sequences analyzed (top, black). Regarding the amino acid coloring pattern, positively charged residues (e.g., arginine and lysine) are colored in red, negatively charged residues (i.e., aspartic and glutamic acid) in blue, polar uncharged residues (i.e., asparagine, glutamine, serine, and threonine) in purple and sky blue, hydrophobic residues (e.g., isoleucine, leucine, and valine) in bright green, aromatic residues (i.e., phenylalanine, tryptophan, and tyrosine) in dark green, and cysteines in yellow. The columns colored in black correspond to gaps in the sequence alignment. Some of the most evolutionarily conserved residues are also color-coded in each of the sequences. In the case of *LiveDrop* **(A)**, the midpoint proline (P185), the positively charged residues (K167, R179, R187), and three of the aromatic residues (W172, Y180, F192) are highlighted. Similarly, in the predicted ALG14 hairpin **(B)**, the midpoint proline (P108), two of the positively charged residues (R105, R107), and three of the aromatic residues (W98, F122, Y124) are highlighted.

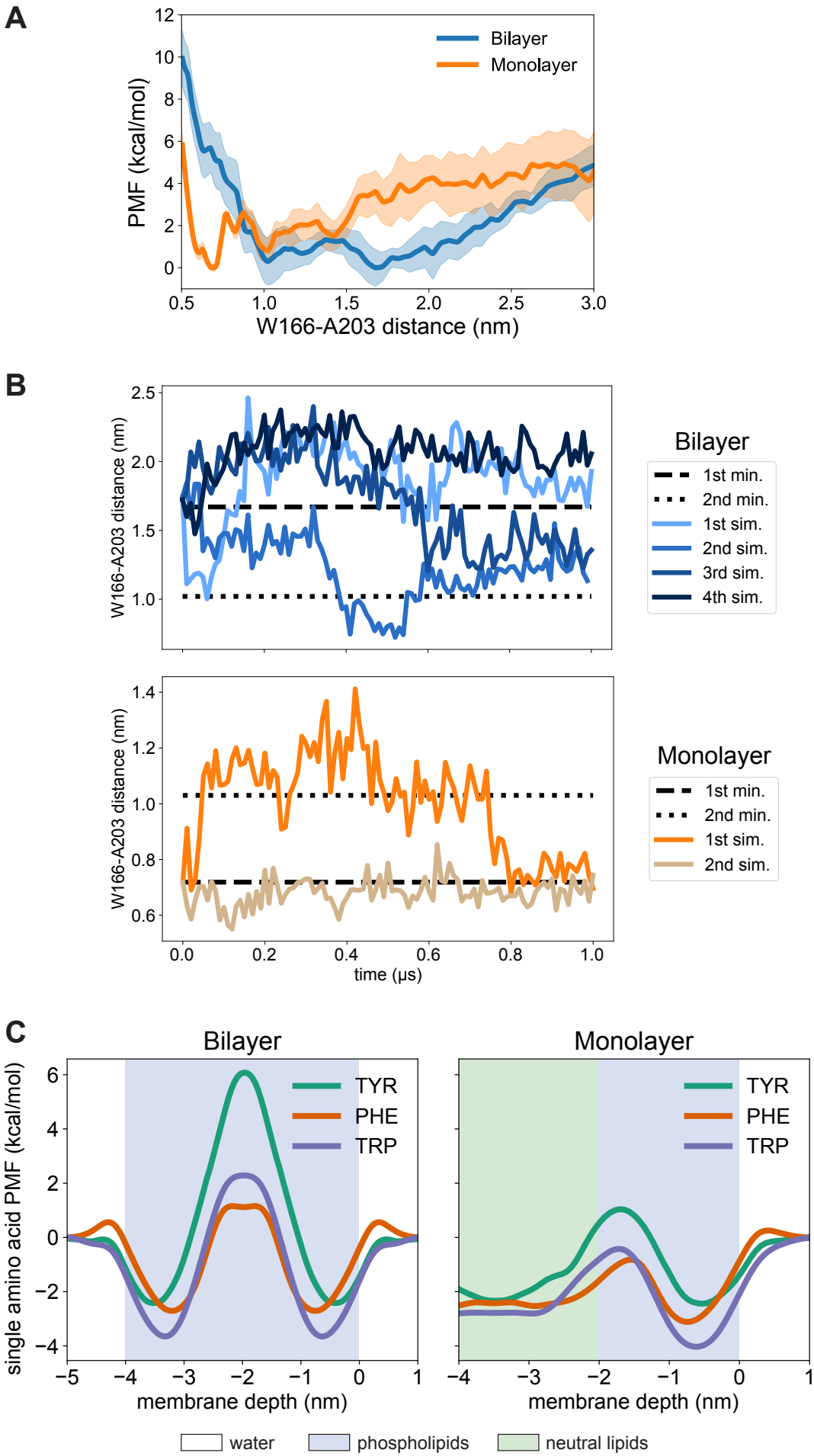
A
Bilayer
Monolayer
PMF (kcal/mol)
W166-A203 distance (nm)
B
W166-A203 distance (nm)
Bilayer
1st min.
2nd min.
1st sim.
2nd sim.
3rd sim.
4th sim.
Monolayer
1st min.
2nd min.
1st sim.
2nd sim.
time (μs)
C
Bilayer
Monolayer
TYR
PHE
TRP
single amino acid PMF (kcal/mol)
membrane depth (nm)
water
phospholipids
neutral lipids

Figure S4 (related to Figure 3). Umbrella sampling simulations of *LiveDrop* and free energy profiles of single amino acids

(A) Potential of mean force (PMF) for the association of the *LiveDrop* α-helices. The distance between residues W166 and A203 (W166-A203 distance), both located close to the top ends of each helix, was used to approximate the degree of proximity between the α-helices of *LiveDrop*. The PMF was calculated as a function of this distance, and the error was estimated using the block averaging method, which entails dividing the equilibrated trajectories into four blocks. The α-helices of *LiveDrop* are closer together in the monolayer (orange), with a minimum in the PMF at 0.7 nm. Conversely, in the bilayer (blue), they are more separated.
(B) Distance between residues W166 and A203 throughout the molecular dynamics simulations (final production run) of *LiveDrop* in the bilayer (upper panel) and monolayer (lower panel). The initial protein structure used in each membrane system was taken from the corresponding umbrella sampling (US) minimum representation. The dashed line is the distance corresponding to the energy minimum in the US calculation, and the dotted line is the distance corresponding to the second energy minimum. As observed in the US result (see Fig. S4A), no significant barrier separates the two most stable states in the bilayer. Thus, the bilayer simulations explore the region broadly where the free energy is not too high. On the other hand, the two most stable states in the monolayer are separated by a 1–2 kcal/mol barrier, and the monolayer simulations mostly sample the first and second stable states.
(C) PMF for the permeation of single phenylalanine (orange), tryptophan (violet), and tyrosine (dark green) residues into the bilayer and monolayer. These free energy profiles, in combination with each residue's specific position (membrane depth) in the dominant bilayer and monolayer conformations, were used to estimate the change in free energy for each residue between the bilayer and monolayer environments. The error (not shown here) was estimated by taking the standard deviation from four independent simulations, resulting in values which were within 1 kcal/mol and 2 kcal/mol for the bilayer and monolayer, respectively.

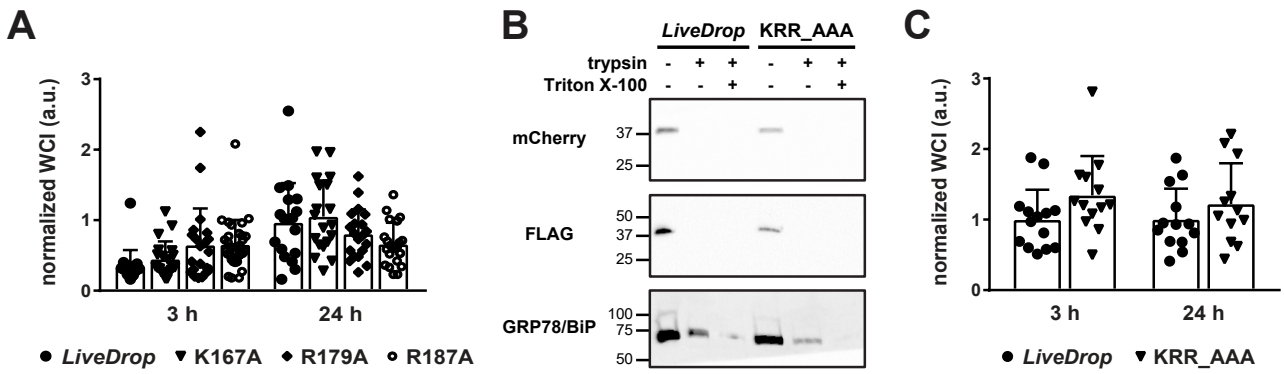

D

LiveDrop FISWKITSIWVFGFFIRYVILMPLRVLVCFVGVVWLTVCTAAVG

FWY→VVV ---V-----V-V-VV--V----------V----V---------

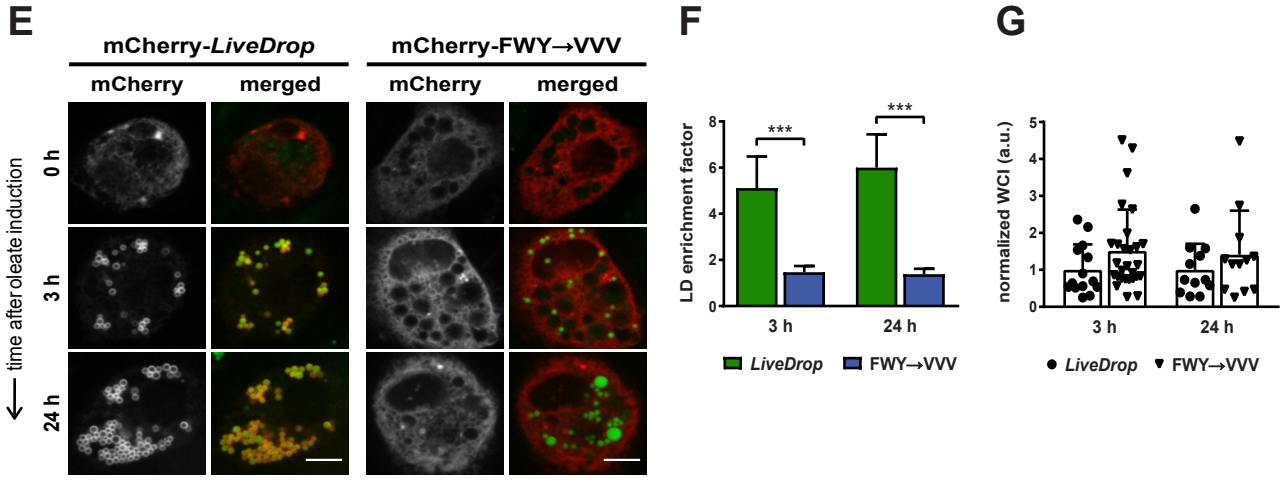

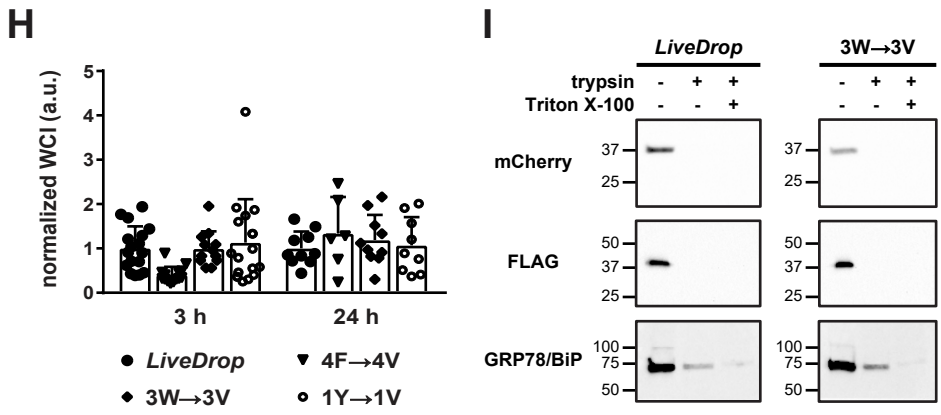

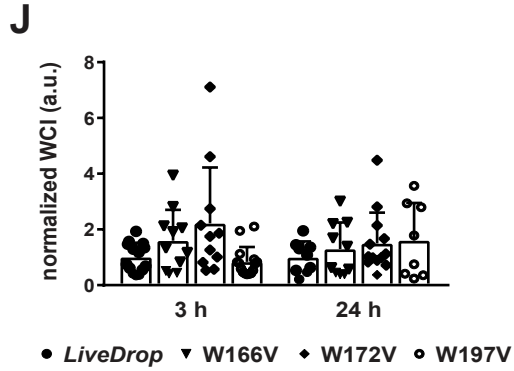

Figure S5 (related to Figure 4). Large hydrophobic residues are required for *LiveDrop* accumulation on LDs

(A) Mean values + SD (n > 18) of the whole-cell protein signals for the cells expressing *LiveDrop* and the variants K167A, R179A, and R187A in Figs. 4A and 4B. Single data points are shown. WCI, whole-cell intensity; a.u., arbitrary units.
(B) Similar to *LiveDrop*, the N- and C-termini of the *LiveDrop* variant with the mutated positively charged residues (KRR_AAA) are exposed to the cytosolic side of the ER membrane.
(C) Mean values + SD (n > 10) of the whole-cell protein signals for the cells expressing *LiveDrop* and the KRR_AAA variant in Figs. 4C and 4D. Single data points are shown. WCI, whole-cell intensity; a.u., arbitrary units.
(D) Amino acid sequence of *LiveDrop* and the FWY→VVV variant, in which the large hydrophobic residues (orange), including phenylalanines, tryptophans, and tyrosines, are mutated to valines. The predicted hinge of the *LiveDrop* sequence (gray) is shown in black. For the FWY→VVV variant, the amino acid positions indicated with a hyphen (–) remain the same as in the original sequence.
(E) Compared to the wild-type *LiveDrop* sequence, the FWY→VVV variant shows abolished LD targeting. *Drosophila* S2 cells transfected with mCherry-tagged versions of *LiveDrop* and the FWY→VVV variant (red) were incubated with oleate throughput the indicated time points and imaged by confocal microscopy. LDs were stained with BODIPY (green). Scale bar, 5 μm.
(F) Mean values + SD (n > 12) of the protein signal on LDs after 3 and 24 h of oleate treatment. ***, $p < 0.001$.
(G) Mean values + SD (n > 12) of the whole-cell protein signal for the cells expressing *LiveDrop* and the FWY→VVV variant in Figs. S5E and S5F. Single data points are shown. WCI, whole-cell intensity; a.u., arbitrary units.
(H) Mean values + SD (n > 10) of the whole-cell protein signals for the cells expressing *LiveDrop* and the variants 4F→4V, 3W→3V, and 1Y→1V in Figs. 4F and 4G. Single data points are shown. WCI, whole-cell intensity; a.u., arbitrary units.
(I) Similar to *LiveDrop*, the N- and C-termini of the *LiveDrop* variant with the mutated tryptophan residues (3W→3V) are exposed to the cytosolic side of the ER membrane. The samples shown in both the right and left panels were ran on the same SDS-PAGE gel.
For **(B)** and **(I)**, microsomal fractions from *Drosophila* S2 cells expressing double-tagged versions of *LiveDrop* (mCherry-*LiveDrop*-FLAG) and each of the respective variants (i.e., mCherry-KRR_AAA-FLAG **(B)** and mCherry-3W→3V-FLAG **(I)**) were treated with 12.5 μg/ml of the protease trypsin in the absence or presence of 1% Triton X-100. Western blot analysis revealed that, for both variants, the mCherry and FLAG tags were fully digested regardless of the presence of Triton X-100, while the ER luminal protein GRP78/BiP (control) only gets fully digested when including Triton X-100.
(J) Mean values + SD (n > 10) of the whole-cell protein signals for the cells expressing *LiveDrop* and the variants W166V, W172V, and W197V in Figs. 4H and 4I. Single data points are shown. WCI, whole-cell intensity; a.u., arbitrary units.

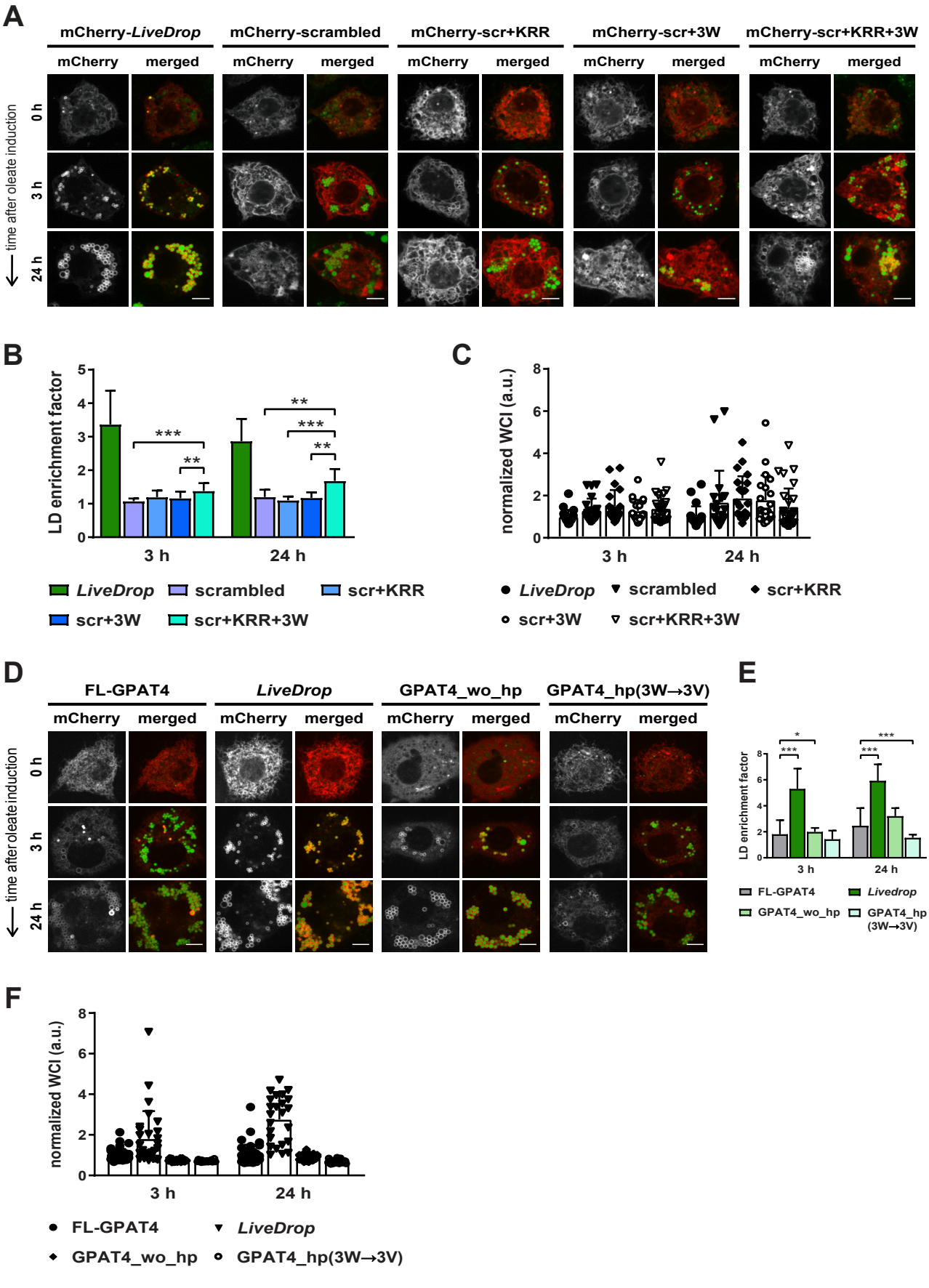
A
mCherry-LiveDrop
mCherry-scrambled
mCherry-scr+KRR
mCherry-scr+3W
mCherry-scr+KRR+3W
mCherry
merged
time after oleate induction
0 h
3 h
24 h
B
LD enrichment factor
3 h
24 h
LiveDrop
scrambled
scr+KRR
scr+3W
scr+KRR+3W
C
normalized WCI (a.u.)
D
FL-GPAT4
LiveDrop
GPAT4_wo_hp
GPAT4_hp(3W→3V)
E
Livedrop
F

Figure S6 (related to Figure 4). Full-length GPAT4 harbors additional sequence determinants outside, and possibly within, the *LiveDrop* motif that contribute to LD accumulation

(A) LD targeting of scrambled *LiveDrop* variants in which the positively charged (K167, R179, R187) and tryptophan residues (W166, W172, W197) have been placed back in their original wild-type position individually (scr+KRR, scr+3W) and in combination (scr+KRR+3W).
(B) Mean values + SD (n > 20) of the protein signal on LDs after 3 and 24 h of oleate treatment. **, $p < 0.01$; ***, $p < 0.001$.
(C) Mean values + SD (n > 20) of the whole-cell protein signals for the cells expressing *LiveDrop*, its scrambled variant, and the scr+KRR, scr+3W, and scr+KRR+3W variants in Figs. S6A and S6B. Single data points are shown. WCI, whole-cell intensity; a.u., arbitrary units.
(D) Besides *LiveDrop*, other sequence motifs of full-length GPAT4 (FL-GPAT4) contribute to its LD targeting. A full-length GPAT4 variant in which the *LiveDrop* motif has been exchanged for a linker sequence (GPAT4_wo_hp) targets LDs from the cytosol. Likewise, disrupting the LD targeting capacity of the *LiveDrop* motif, by exchanging its tryptophan residues for valines, in the background of full-length GPAT4 (GPAT4_hp(3W→3V)) causes a reduction in LD accumulation from the ER at late time points of LD induction.
(E) Mean values + SD (n > 20) of the protein signal on LDs after 3 and 24 h of oleate treatment. *, $p < 0.05$; ***, $p < 0.001$.
(F) Mean values + SD (n > 20) of the whole-cell protein signals for the cells expressing FL-GPAT4, *LiveDrop*, and the indicated GPAT4 variants in Figs. S6D and S6E. Single data points are shown. WCI, whole-cell intensity; a.u., arbitrary units.
For **(A)** and **(D)**, *Drosophila* S2 cells were transfected with mCherry-tagged versions of each of the *LiveDrop* and GPAT4 variants (red), incubated with oleate throughout the indicated time points, and imaged by confocal microscopy. LDs were stained with BODIPY (green). Scale bar, 5 µm.

A

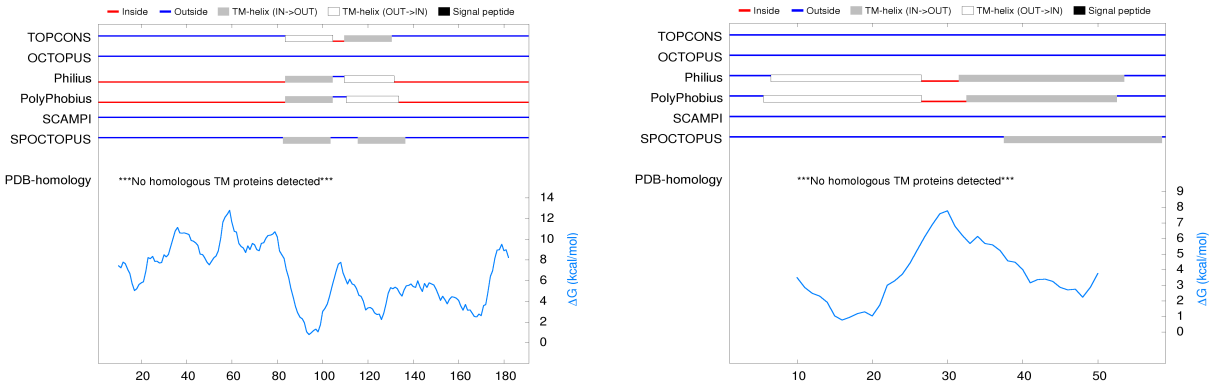

B

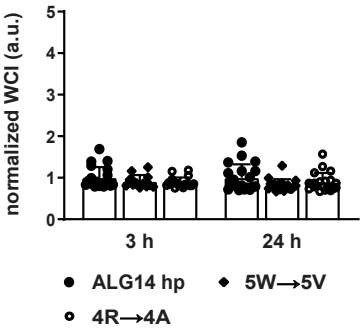

C

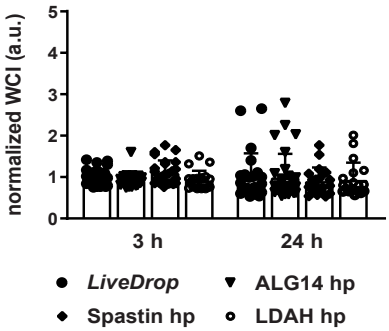

D

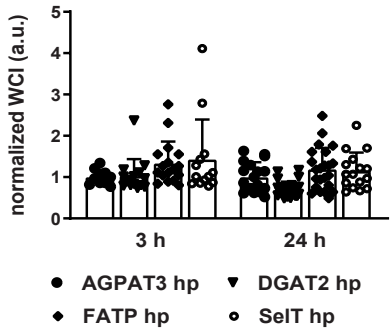

E

LiveDrop	FISWKITSIWVFGFFIRYVILMPLRVLVCFVGVVWLTVCTAAVG
ALG14 hp	WLSSIFTSLWALLWSCYLVWRDRPQLILCNGPGTCVPFCYAAYLWRLLGRL
Spastin hp	LYVVSFPIIFLFNVLRSLIYQLFCIFRYLYG
LDAH hp	WVFTKVAMPLYSVFGYIFFSFFNFLPVWLRLMLIQIYFLIFSIPRQFL

F

AGPAT3 hp	LVNFVCWAVFSLSCIFYYVITSLLAANWTAFITALSVLGLFYWLM
DGAT2 hp	ILVTAFFTSMLLILLSVSFLLVAGSLIYGGLLVRSLMVTYLAYVFVH
FATP hp	FLVIFRFFCATVAFGLAIACVIYTLHTMGWIFAVLVALVALLLTKPGWRWF
SelT hp	GLNYYLSKMIFALKIIIIVSVVSAVSPFTFLGLNTPSWWSHMQANKIYACMMIFFLGNMLEAQLIS

G

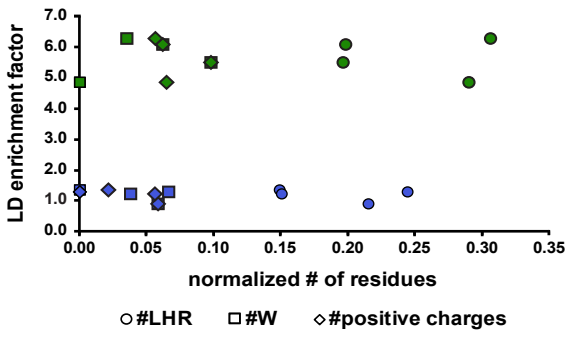

H

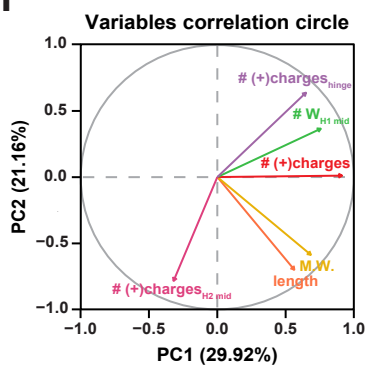

Figure S7 (related to Figures 5 and 6). Secondary structure prediction of ALG14 and sequence analysis of the LD targeting and non-LD targeting motifs

(A) Secondary structure predictions of *D. melanogaster* ALG14 (1–191 aa, left) and its predicted hairpin motif (83–137 aa, right). TOPCONS (http://topcons.cbr.su.se/) was used to predict the transmembrane (TM) domains in both sequences. The results also include the predictions from additional bioinformatics tools, such as OCTOPUS, Philius, PolyPhobius, SCAMPI, and SPOCTOPUS. The predicted TM domains are depicted as white and gray bars, based on their membrane orientation, and the sequence regions predicted to be non-TM are represented as solid lines. The results of comparing each sequence to the PDB (Protein Data Bank), as well as the respective free energy (ΔG kcal/mol) profiles (blue trace), are shown at the bottom of each panel.
(B) Mean values + SD (n > 13) of the whole-cell protein signals for the cells expressing the predicted ALG14 hairpin (ALG14 hp) and its sequence variants 5W→5V and 4R→4A in Figs. 5E and 5F. Single data points are shown. WCI, whole-cell intensity; a.u., arbitrary units.
(C) Mean values + SD (n > 19) of the whole-cell protein signals for the cells expressing *LiveDrop* and the predicted hairpin motifs of ALG14 (ALG14 hp), spastin (spastin hp) and LDAH (LDAH hp) in Figs. 6A and 6B. Single data points are shown. WCI, whole-cell intensity; a.u., arbitrary units.
(D) Mean values + SD (n > 10) of the whole-cell protein signals for the cells expressing the predicted hairpin motifs of AGPAT3 (AGPAT3 hp), DGAT2 (DGAT2 hp), FATP (FATP hp), and SelT-like protein (SelT hp) in Figs. 6C and 6D. Single data points are shown. WCI, whole-cell intensity; a.u., arbitrary units.
(E) Amino acid sequences of the identified LD targeting motifs, including *LiveDrop* and the predicted hairpin motifs of ALG14 (ALG14 hp), spastin (spastin hp) and LDAH (LDAH hp). In all cases, the predicted hinge is shown in black. Further information regarding the specific protein isoform and amino acid sequence range used is shown in Table 2.
(F) Amino acid sequences of the identified non-LD targeting motifs, including the predicted hairpin motifs of AGPAT3 (AGPAT3 hp), DGAT2 (DGAT2 hp), FATP (FATP hp), and SelT-like protein (SelT hp). Further information regarding the specific protein isoform and amino acid sequence range used is shown in Table 2.
(G) Plot of the normalized number of large hydrophobic residues (LHR, ○), tryptophan residues (W, □), and positive charges (◊), calculated in Table S1, against the LD enrichment factors measured for the LD targeting (green data points) and non-LD targeting (violet data points) motifs. The number of either LD targeting feature in the sequences analyzed does not correlate with their respective LD targeting capacities.
(H) Correlation plot between the variables included in the principal component analysis (PCA) and the first two principal components (PC1 and PC2). The variables were ranked based on the extent of their contribution to the variance explained by PC1 and PC2. Only the variables ranked among the top six, including the total number of positive charges [# (+)charges], the number of positive charges at the hairpin hinge [# $(+)charges_{hinge}$], and the number of tryptophans within the middle section of the first helix [# W_{H1mid}], are shown. Each variable is represented as an individual vector, and their closeness to the circumference of the correlation circle (gray) is proportional to their degree of representation in the PCs.

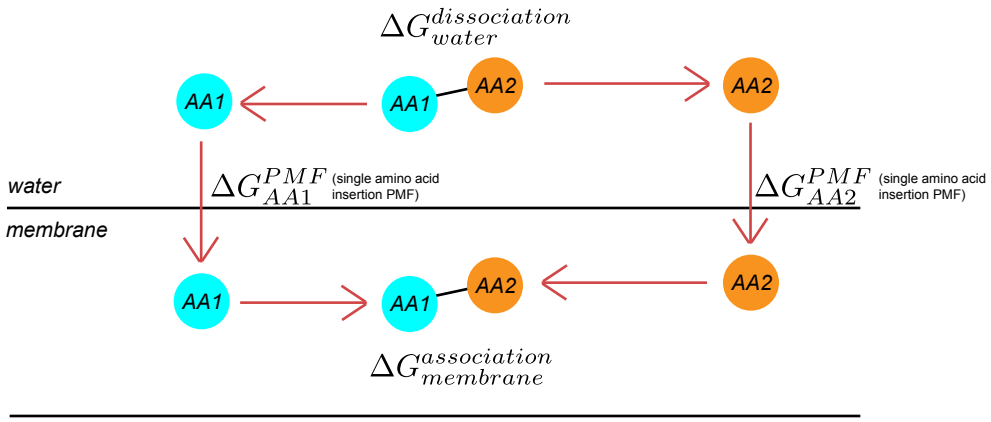

$$\Delta G(BI) = \Delta G^{dissociation}_{water}(BI) + \Delta G^{PMF}_{AA1}(BI) + \Delta G^{PMF}_{AA2}(BI) + \Delta G^{association}_{membrane}(BI)$$
$$\Delta G(LD) = \Delta G^{dissociation}_{water}(LD) + \Delta G^{PMF}_{AA1}(LD) + \Delta G^{PMF}_{AA2}(LD) + \Delta G^{association}_{membrane}(LD)$$

$$if\ \Delta G^{association}_{membrane}(BI) = \Delta G^{association}_{membrane}(LD),$$
$$\Delta G(BI) - \Delta G(LD) = (\Delta G^{PMF}_{AA1}(BI) - \Delta G^{PMF}_{AA1}(LD)) + (\Delta G^{PMF}_{AA2}(BI) - \Delta G^{PMF}_{AA2}(LD))$$

Figure S8 (related to STAR Methods). Thermodynamic cycle for the membrane insertion of a single amino acid

Diagram describing the insertion free energy of a peptide (ΔG) in terms of the insertion free energy of a single amino acid ($\Delta G^{\mathrm{PMF}}_{\mathrm{AA}}$), similar to the permeation free energy profiles calculated in Figure S4C. In this thermodynamic cycle, a peptide, consisting of two amino acids (AA1–AA2) but extendable to a longer peptide, disassociates in water ($\Delta G^{\mathrm{dissociation}}_{\mathrm{water}}$). Each single residue (AA1, AA2) inserts into the bilayer (BI) or LD monolayer ($\Delta G^{\mathrm{PMF}}_{\mathrm{AA}}$), and subsequently associates with each other (AA1–AA2) once they are both in the bilayer or monolayer environment ($\Delta G^{\mathrm{association}}_{\mathrm{membrane}}$). It is reasonable to assume that the free energy for two single amino acids to associate in the monolayer or in the bilayer is minimally different. Therefore, the free energy difference for the peptide to insert into the bilayer versus the monolayer is mainly dictated by the difference between the insertion free energies of each amino acid, as shown in the final equation.

SUPPLEMENTAL TABLES

Table S1 (related to Figure 6). Normalized number of LD targeting sequence features									
Type of motif	**Predicted hairpins**	**LD enrichment factor**	**Length (aa)**	**#LHR**	**#LHR_n**	**#W**	**#W_n**	**#positive charges**	**#positive charges_n**
LD targeting	*LiveDrop*	6.12	44	9	0.20	3	0.07	3	0.07
	ALG14 hp	5.53	51	10	0.20	5	0.10	5	0.10
	Spastin hp	4.88	31	9	0.29	0	0.00	2	0.06
	LDAH hp	6.29	48	15	0.31	2	0.04	3	0.06
non-LD targeting	AGPAT3 hp	1.31	45	11	0.24	3	0.07	0	0.00
	DGAT2 hp	1.37	47	7	0.15	0	0.00	1	0.02
	FATP hp	0.92	51	11	0.22	3	0.06	3	0.06
	SelT hp	1.25	53	8	0.15	2	0.04	3	0.06

The total number of large hydrophobic (#LHR), tryptophan (#W), and positively charged residues, per predicted hairpin motif, was divided by the corresponding sequence length, resulting in normalized values ('n' columns) for the number of these sequence features.

Table S2 (related to Figure 6). Matrix of variables used for principal component analysis (PCA)											
Type of motif	**Predicted hairpins**	**Length (aa)**	**M.W.**	**pI**	**H**	**μ**	**#pos charges**	**#neg charges**	**Net charge**	**#LHR**	**#W**
LD targeting	*LiveDrop*	44	5052.26	9.5	1.063	0.056	3	0	3	9	3
	ALG14 hp	51	6023.19	8.92	0.91	0.158	5	1	3	10	5
	Spastin hp	31	3821.67	9.11	1.071	0.298	2	0	2	9	0
	LDAH hp	48	5961.3	9.99	1.085	0.215	3	0	3	15	2
non-LD targeting	AGPAT3 hp	45	5172.23	5.51	1.088	0.105	0	0	0	11	3
	DGAT2 hp	47	5166.38	8.5	1.01	0.019	1	0	1	7	0
	FATP hp	51	5808.18	9.5	1.053	0.062	3	0	3	11	3
	SelT hp	53	6025.4	9.63	0.872	0.084	3	0	3	8	2

Type of motif	**Predicted hairpins**	**N° of tryptophans**					**N° of positive charges**				
		H1 top	**H1 mid**	**Hinge**	**H2 mid**	**H2 top**	**H1 top**	**H1 mid**	**Hinge**	**H2 mid**	**H2 top**
LD targeting	*LiveDrop*	1	1	0	1	0	1	1	1	0	0
	ALG14 hp	1	2	1	0	1	0	0	2	0	2
	Spastin hp	0	0	0	0	0	0	0	1	0	1
	LDAH hp	1	0	1	0	0	1	0	1	0	1
non-LD targeting	AGPAT3 hp	1	0	1	0	1	0	0	0	0	0
	DGAT2 hp	0	0	0	0	0	0	0	0	1	0
	FATP hp	0	0	1	0	2	1	0	0	0	2
	SelT hp	0	0	2	0	0	2	0	0	1	0

Sequence analysis of the predicted hairpins classified as LD targeting and non-LD targeting motifs yielded a set of parameters that were used as variables for PCA. These included physicochemical parameters (upper part), such as molecular weight (M.W.), isoelectric point (pI), hydrophobicity (H), and hydrophobic moment (μ), and some sequence-derived parameters (upper part), such as the number of positively (#pos charges) and negatively (#neg charges) charged residues, the number of large hydrophobic residues (#LHR), and the number of tryptophans (#W). Residue distribution variables (lower part), corresponding to the number of tryptophan and positively charged residues per each hairpin region (see Table 1 for details), were also included in the PCA. H1 top, top region of helix 1; H1 mid, middle region of helix 1; H2 mid, middle region of helix 2; H2 top, top region of helix 2.

Table S3 (related to STAR Methods). List of plasmids used in this study		
Plasmid name	**Insert generation strategy**	**Vector backbone**
mCherry-GPAT4	Wilfling et al., 2013	pA-CherryW
mCherry-*LiveDrop*	Wilfling et al., 2013	pA-CherryW
mCherry-*LiveDrop*-mCherry	PCR	pA-CherryW
mCherry-GPAT4 ΔC	Farese & Walther lab collection	pA-CherryW
mCherry-GPAT4 ΔN	Farese & Walther lab collection	pA-CherryW
mCherry-*LiveDrop*_Δ4 AAs	synthetic double-stranded DNA	pA-CherryW
mCherry-*LiveDrop*_MP_VV	site-directed mutagenesis	pA-CherryW
mCherry-*LiveDrop*-FLAG	synthetic double-stranded DNA	pA-CherryW
mCherry-scrambled	synthetic double-stranded DNA	pA-CherryW
mCherry-scrambled-FLAG	synthetic double-stranded DNA	pA-CherryW
mCherry-synthetic	synthetic double-stranded DNA	pA-CherryW
mCherry-synthetic-FLAG	synthetic double-stranded DNA	pA-CherryW
mCherry-*LiveDrop*_K167A	site-directed mutagenesis	pA-CherryW
mCherry-*LiveDrop*_R179A	site-directed mutagenesis	pA-CherryW
mCherry-*LiveDrop*_R187A	site-directed mutagenesis	pA-CherryW
mCherry-*LiveDrop*_KRR_AAA	synthetic double-stranded DNA	pA-CherryW
mCherry-KRR_AAA-FLAG	synthetic double-stranded DNA	pA-CherryW
mCherry-*LiveDrop*_FWY→VVV	synthetic double-stranded DNA	pA-CherryW
mCherry-*LiveDrop*_4F→4V	synthetic double-stranded DNA	pA-CherryW
mCherry-*LiveDrop*_3W→3V	synthetic double-stranded DNA	pA-CherryW
mCherry-3W→3V-FLAG	synthetic double-stranded DNA	pA-CherryW
mCherry-*LiveDrop*_1Y→1V	site-directed mutagenesis	pA-CherryW
mCherry-*LiveDrop*_W166V	site-directed mutagenesis	pA-CherryW
mCherry-*LiveDrop*_W172V	site-directed mutagenesis	pA-CherryW
mCherry-*LiveDrop*_W197V	site-directed mutagenesis	pA-CherryW
mCherry-scr+KRR	synthetic double-stranded DNA	pA-CherryW
mCherry-scr+3W	synthetic double-stranded DNA	pA-CherryW
mCherry-scr+KRR+3W	synthetic double-stranded DNA	pA-CherryW
mCherry-GPAT4_wo_hp	Wilfling et al., 2013	pA-CherryW
mCherry-GPAT4_hp(3W→3V)	synthetic double-stranded DNA	pA-CherryW
mCherry-ALG14 hp	synthetic double-stranded DNA	pA-CherryW
mCherry-ALG14 hp_5W→5V	synthetic double-stranded DNA	pA-CherryW
mCherry-ALG14 hp_4R→4A	synthetic double-stranded DNA	pA-CherryW
mCherry-Spastin hp	synthetic double-stranded DNA	pA-CherryW
mCherry-LDAH hp	synthetic double-stranded DNA	pA-CherryW
mCherry-AGPAT3 hp	synthetic double-stranded DNA	pA-CherryW
mCherry-DGAT2 hp	synthetic double-stranded DNA	pA-CherryW
mCherry-FATP hp	synthetic double-stranded DNA	pA-CherryW
mCherry-SelT hp	synthetic double-stranded DNA	pA-CherryW

Table S4 (related to STAR Methods). Sequences of primers used for site-directed mutagenesis

Plasmid generated	Forward	Reverse
mCherry-*LiveDrop*_MP_VV	CTACGTCATCCTGGTGGTCCTCCGGGTATTGG	CCAATACCCGGAGGACCACCAGGATGACGTAGC
mCherry-*LiveDrop*_K167A	GAGTTCATTTCCTGGGCAATCACCTCCATCTGGG	CCAGATGGAGGTGATTGCCCAGGAAATGAACTCG
mCherry-*LiveDrop*_R179A	GCTTCTTCATCGCCTACGTCATCCTGATGCC	CATCAGGATGACGTAGGCGATGAAGAAGCCG
mCherry-*LiveDrop*_R187A	CCTGATGCCCCTCGCGGTATTGGTATGCTTCG	GAAGCATACCAATACCGCGAGGGGCATCAGG
mCherry-*LiveDrop*_1Y→1V	GCTTCTTCATCCGCGTCGTCATCCTGATGCC	GGCATCAGGATGACGACGCGGATGAAGAAGC
mCherry-*LiveDrop*_W166V	ACGAGTTCATTTCCGTGAAAATCACCTCCATCTGG	CCAGATGGAGGTGATTTTCACGGAAATGAACTCGT
mCherry-*LiveDrop*_W172V	AAATCACCTCCATCGTGGTGTTCGGCTTCTTC	GAAGAAGCCGAACACCACGATGGAGGTGATTT
mCherry-*LiveDrop*_W197V	TCGTTGGTGTAGTGGTGTTAACAGTCTGCACG	CGTGCAGACTGTTAACACCACTACACCAACGA

Table S5 (related to STAR Methods). Summary of simulations and lipid compositions used							
Protein	**Membrane system**	**Simulation type**	N^u_{POPC}: N^u_{DOPE}: N^u_{SAPI}	N^l_{POPC}: N^l_{DOPE}: N^l_{SAPI}	N_{TG}: N_{CLOL}	**#**	**Time (ns)**
LiveDrop	bilayer	US	130:54:16	128:53:16	0:0	80	50–90
LiveDrop	monolayer	US	110:46:13	108:45:13	91:92	80	50–90
LiveDrop	bilayer	MD	133:55:16	138:56:16	0:0	4	1000
LiveDrop	monolayer	MD	130:54:16	136:57:17	651:0	2	1000
ALG14 hp	bilayer	MD	134:55:16	133:55:16	0:0	2	2000
ALG14 hp	bilayer	MD	134:55:16	134:55:16	0:0	2	2000
ALG14 hp	monolayer	MD	134:55:16	136:57:17	638:0	2	2000
ALG14 hp	monolayer	MD	134:55:16	136:57:17	640:0	2	2000

List of each type of simulation performed for *LiveDrop* and the predicted ALG14 hairpin (ALG14 hp) in both the bilayer and monolayer systems. 'N^u' and 'N^l' represent the number of molecules in the upper and lower phospholipid leaflets, respectively. The '**#**' column represents the number of windows used in the umbrella sampling (US) simulations and the number of duplicates in the case of the molecular dynamics (MD) simulations. CLOL, cholesteryl oleate.